Nylon 6,6 electrospun fibres reinforced by amino functionalised 1D and 2D carbon

Nylon 6,6 electrospun fibres reinforced by amino functionalised 1D and 2D carbon

F Navarro-Pardo[1,2], G Martínez-Barrera[1], A L Martínez-Hernández[2,3], V M Castaño[2], J L Rivera-Armenta[4], F Medellín-Rodríguez[5], C Velasco-Santos[2,3,6]

[1]Universidad Autónoma del Estado de México, Facultad de Química, Laboratorio de Investigación y Desarrollo de Materiales Avanzados, Km. 12 de la carretera Toluca-Atlacomulco, C.P. 50200, San Cayetano, Toluca, Estado de México, México.

[2]Universidad Nacional Autónoma de México, Centro de Física Aplicada y Tecnología Avanzada, Boulevard Juriquilla No. 3001, C.P. 76230, Santiago de Querétaro, Querétaro, México.

[3]Instituto Tecnológico de Querétaro, División de Estudios de Posgrado e Investigación, Av. Tecnológico s/n, esq. Gral. Mariano Escobedo, Col. Centro Histórico, C.P. 76000, Santiago de Querétaro, Querétaro, México.

[4]Instituto Tecnológico de Ciudad Madero, División de Estudios de Posgrado e Investigación, Juventino Rosas y Jesús Ureta, Col. Los Mangos, C.P. 89440, Ciudad Madero, Tamaulipas, México.

[5]Universidad Autónoma del San Luis Potosí, Facultad de Ciencias Químicas, Av. Manuel Nava 6, Zona Universitaria, C.P. 78210, San Luis Potosí, San Luis Potosí, México.

[6]E-mail address: cylaura@gmail.com

Abstract. Nylon 6,6 electrospun nanocomposites were prepared and reinforced with 0.1, 0.5 and 1wt.% of 1D and 2D carbon. Both carbon nanotubes and graphene were functionalised with amino groups (f-CNT and f-Ge respectively). The morphology and graphitization changes of carbon nanomaterials were evaluated by transmission electron microscopy (TEM) and Raman spectroscopy; functional groups of modified nanomaterials was analysed by infrared spectroscopy. The mechanical response and the crystallinity of the fibres were measured by dynamical mechanical analysis, differential scanning calorimetry and wide angle x-ray diffraction. The morphology and dispersion of the nanomaterials in the nanofibres was studied by scanning electron microscopy and TEM. The storage modulus was improved by 118% for f-CNT and 116% for f-Ge. The mechanical response of the nanocomposites exhibited different behaviour upon loading of 1D and 2D carbon. This trend is consistent with the crystallinity of the nanofibres. This study showed f-CNT resulted in better mechanical properties at the lowest loading. On the other hand f-Ge showed improved reinforcing effect by increasing the filler loading. The two-dimensional structure of graphene was an important factor for the higher crystallinity in the electrospun nanofibres.

1. Introduction

The recent discoveries of 1D and 2D carbon structures have attracted the attention to carbon based nanocomposites. The use of these nanomaterials with improved physicochemical properties has

generated a wide variety of research concerning the fabrication and properties of the resulting nanocomposites [1-3]. One-dimensional carbon nanotubes (CNTs) are considered as a graphene sheet rolled into a cylindrical shape. Two-dimensional graphene is built from a hexagonal array of sp^2 carbon atoms.

Pristine nanometric carbon is extremely difficult to disperse and align in a polymer matrix [1]. Functionalisation provides efficient stress transfer from the polymer matrix to the nanometric carbon by preventing aggregation of them, providing a better dispersion of the nanomaterials in the polymer matrix [4-7]. It also increases the polymer–nanomaterial physical contact and can form chemical bonds between the nanomaterial and the polymer matrix [4].

Nylon 6,6 is a semicrystalline polymer suitable for electrospinning processing. This approach is a simple and versatile method to produce micro to nanometric fibres [8]. Electrospinning offers the possibility to incorporate nanomaterials to fibres [9].

This work presents the reinforcement effect provided by 1D and 2D functionalised carbon to electrospun nanofibres in order to find the features this two different structures and functionalisation provide to the nanocomposites obtained. A relationship between the crystallinity properties found in the nanocomposites is also presented.

2. Experimental work

2.1. Amino functionalisation
Chemical vapour deposition multiwalled carbon nanotubes (Sunnano Company), with 10-30 nm in outer diameter, 1-10 μm length and purity above 80%, were refluxed for three hours at 80ºC in a 3:1 molar solution of nitric acid (HNO$_3$,70%, Sigma-Aldrich) and sulphuric acid (H$_2$SO$_4$, 98%, J.T. Baker). The solution was filtered and washed with distilled water until neutral pH. The oxidised CNTs were dried overnight at 80°C.

Graphene oxide (GO) was prepared by oxidation of graphite using the modified Hummers method as described elsewhere [10, 11]. The graphite oxide was dried overnight at 60°C. The obtained powder was re-dispersed into water and sonicated for three hours in an ultrasound bath in order to obtain graphene oxide. The GO was filtered and dried overnight at 60°C.

An acid–base titration with sodium hydroxide (NaOH, 98%, Sigma-Aldrich) was used to determine the concentration of acidic surface groups [12]. The oxidised carbon materials were added into a 25 ml of a 0.04 N NaOH solution and stirred for 48 h to allow the solid material to equilibrate with the basic solution. The mixture was titrated with a 0.04 N HCl solution to determine the excess NaOH in the solution and the concentration of the carboxylates on CNTs and GO. The concentrations of acidic surface sites were 6.5 mmol/g in the oxidised CNT and 5.4 mmol/g in the GO. The nanomaterials were functionalised as follows: a solution of 1:1 molar ratio of carbon material and 1-ethyl-3-[3-dimethylaminopropyl]carbodiimide hydrochloride) (EDAC, 99%, Sigma Aldrich) was kept under stirring at 80°C in dymethilamine excess for 6 h. The material obtained was washed until neutral pH and dried overnight at 60°C. The functionalised carbon nanotubes and graphene were labelled as f-CNT and f-Ge respectively.

2.2. Polymer solution preparation
The polymer solution was obtained by dissolving 5.5 g of nylon 6,6 (Ultramid® A3K, BASF) in 20 g of formic acid for two hours at 70°C. Afterwards the filler was added and stirred for two hours more. Three filler loadings were chosen: 0.1, 0.5 and 1 wt. %.

2.3. Electrospinning

The polymer solution was fed into a 5 ml syringe (21 gauge 1" needle). The flow rate of the solution was controlled using a syringe pump and kept constant at 5 ml/hr. A voltage of 20 kV was applied directly to the needle; the tip-collector distance was 15 cm. A grounded copper collecting screen was used. The nanocomposites were labelled by the weight percent of the filler followed by the nomenclature of the carbon nanomaterials.

2.4. Characterisation

The carbon nanomaterials were analysed by Fourier transform infrared (FTIR) spectroscopy on a Bruker Optics Vector 33 spectrometer. Raman measurements were obtained using a Dylor LabRaman II with an excitation line of 632.8 nm. Transmission electron microscopy (TEM) micrographs of the carbon nanomaterials and nanocomposites were taken on a JEOL TEM 1010 microscope operating at 80 kV.

The thermo-mechanical response of the nanocomposites was measured using a dynamic mechanical analyser (DMA), TA Instruments DMA 2980. The analyses were performed on samples of $30x5x0.05$ mm^3 under tension film mode in a temperature range of room temperature to 200 °C at a frequency of 1 Hz and a heating rate of 5°/min.

The crystallinity properties were obtained in a differential scanning calorimeter (DSC), Perkin Elmer DSC-7. The samples were heated up to 280°C for five minutes and then they were cooled at 10°C/min. Wide angle X-ray diffraction (WAXD) patterns were obtained in PANalytical X'Pert Pro X-ray diffraction equipment with Cu Kα radiation (k =0.154 nm). The scanning rate was 0.05°/s.

3. Results and discussion

Figure 1a shows the amino functionalised carbon materials. The peaks between 750 cm^{-1} and 980 cm^{-1} in the spectra are due to the wagging of the N-H bond. The C-N stretching is seen ~1220 cm^{-1} [4]. The amide group (C=O) N-H features ~1700 cm^{-1} [5]. This is also related to the in-plane amide N-H deformation mode at ~1570 cm^{-1} [6]. The N-H bend of Amide I is seen at ~1641 cm^{-1} and the N-H stretching at ~1740 cm^{-1} [5]. The peaks at ~1400 cm^{-1} and ~1450 cm^{-1} are due to the attachment of additional methyl groups, attributed by the asymmetric bending of CH$_3$ groups and the peaks at ~2850 and ~2920 cm^{-1} corresponding to the C-H stretching vibration [7].

The usual characteristics of carbon materials in Raman spectra are the G band (~1580 cm^{-1}), which is usually attributed to the E$_{2g}$ phonon of C sp^2 atoms, and the D band (~1320 cm^{-1}) as a breathing mode of κ-point phonons of A$_{1g}$ symmetry, which is attributed to local defects and disorders, particularly located at the edges of graphene [13]. The Raman spectra of f-CNT and f-Ge are shown in figure 1b. Both materials display the G and D bands. Moreover a major fingerprint of graphene is the D' peak at ~2700 cm^{-1}.

The morphology of the carbon materials is shown in the figure 2. In f-CNT is possible to observe a rough surface on the walls of the tubes. In the f-Ge, a mixture of graphene layers is observed; the sheets are rippled and entangled with each other like a silk weave form. Figure 2 also shows the micrographs of the nanofibres at the maximum filler loading. Electrospinning technique is known for the alignment of the nanomaterials along the fibre [9]. Polymer nanocomposites require homogeneous dispersion and strong interfacial interaction between carbon nanomaterials and the polymer matrix for the enhancement of the mechanical and thermal properties [1-7]. Functionalisation is expected to reduce agglomeration of the nanotubes. However at high loading the f-CNT agglomerated showing poor dispersion of the nanotubes. In contrast, at the same loading a graphene sheet is seen embedded

and aligned along the fibre axis showing the good affinity between the polymer matrix and the f-Ge. The agglomeration at high loading of f-CNT in the nanocomposites could be explained by the one-dimensional structure of the nanotubes that allows them to easily bend and interact with the amino groups on their surface.
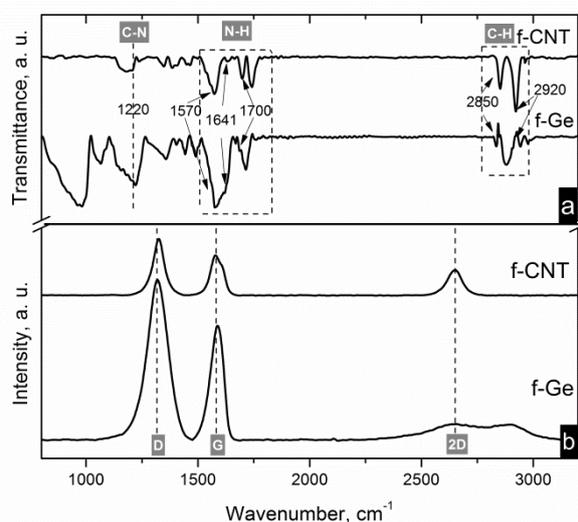

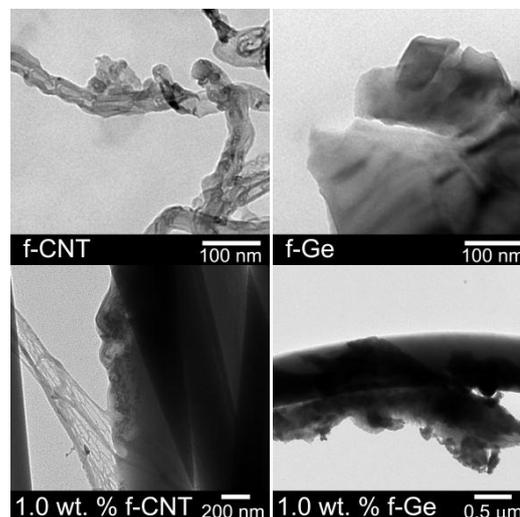**Figure 1.** a) IR and b) Raman spectra, of the carbon nanomaterials.

Figure 2. TEM micrographs of the carbon nanomaterials and nanocomposites.

Figure 3 shows the SEM images of the electrospun nanofibres oriented randomly in a non-women mat. Uniform fibres with no beads were obtained. The nanometric carbon embedded within the fibres is not visible. However the deposited carbon materials on the surface of the fibres are observed in the bright areas of the images.
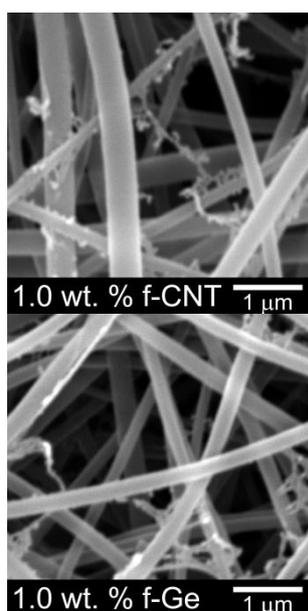

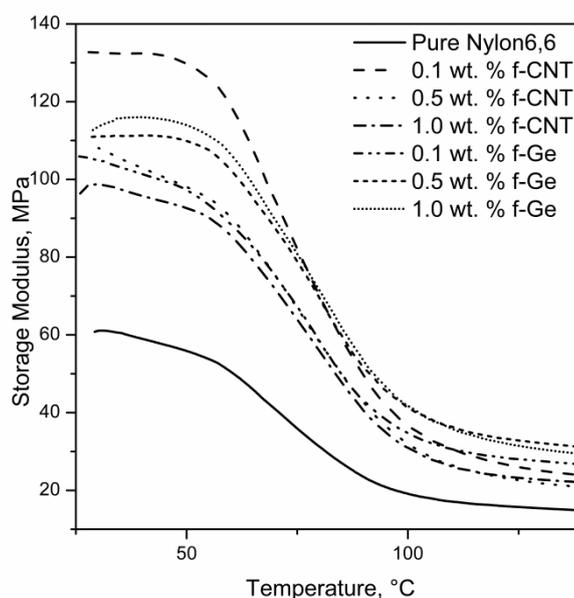**Figure 3.** SEM photographs of nanocomposites.

Figure 4. Storage modulus of the pure nylon 6,6 nanofibres and nanocomposites.

The storage modulus of pure nylon 6,6 and the nanocomposites is presented in figure 4. The improved mechanical response of the nanofibres is due to the strengthening effect of the carbon nanomaterials [1]. At the lowest loading of f-CNT the modulus reaches a 118% increase compared to pure nylon 6,6 nanofibres. However when the filler loading is increased this property is decreased. This behaviour can be attributed to agglomeration of the nanotubes in the nanofibre, as seen in Figure 2. On the other hand the storage modulus in the f-Ge reinforced composites showed a tendency to increase as the loading of the filler increased. The modulus was improved from a 70% for a 0.1 wt. % to a 116% for the maximum loading of f-Ge. The values of the glass transition temperature in table 1 were obtained from tan δ peak maximum of the DMA. This property was enhanced up to 7°C for the f-CNT nanocomposites and up to 5°C for the f-Ge nanocomposites at the highest loading.

Crystallinity and molecular orientation provide unique physical features to the nanocomposites and play an important role in mechanical properties of the fibres [14]. The crystallinity properties of the nanofibres are also displayed in table 1. The degree of crystallinity (X_C) was calculated from the heating thermograms of DSC [15] and the crystallinity index (CI) from the WAXD patterns. The crystal sizes L_1 and L_2 were obtained applying the Scherrer equation to the two diffraction signals of the nylon 6,6 that are a project value of the interchain distance within the hydrogen-bonded sheet (L_1) and the the intersheet distance (L_2) [16].This results are associated with the effect imparted by the carbon nanomaterials on the crystal structure and hence with the mechanical response of the nanocomposites. The crystallinity in the f-CNT reinforced nanofibres decreases as the filler content increases .The opposite behaviour is observed in the f-Ge based nanofibres. This is in agreement with Wong et al. who found that a higher degree of crystallinity and molecular orientation of fibres resulted in improved mechanical strength and stiffness [8]. Moreover, the crystal sizes of the nanocomposites are in accordance with these results. This means the carbon nanomaterials with a high nucleation density provide more defects in the crystal indicating lower crystal perfection [14]. The better dispersion in f-Ge resulted in smaller crystal size of the nanocomposites.

Table 1. Crystallinity, crystal size and glass temperature of the nanocomposites.

Nanofibres	X_c, %	CI	L_1, nm	L_2, nm	T_g, °C
Nylon 6,6	39.38	0.383	6.451	3.410	79
0.1 wt. % f-CNT	44.31	0.435	5.350	3.105	83
0.5 wt. % f-CNT	38.90	0.390	5.930	3.233	85
1.0 wt. % f-CNT	41.13	0.388	5.982	3.880	86
0.1 wt. % f-Ge	41.12	0.403	6.291	2.974	83
0.5 wt. % f-Ge	41.73	0.417	5.667	3.187	84
1.0 wt. % f-Ge	43.09	0.431	5.763	2.848	84

4. Conclusion

The electrospun nanocomposites obtained in this work showed the different behaviour of functionalised 1D and 2D carbon at different loadings. One of the findings of the study between the two structures of the fillers was the one-dimensionality of the f-CNT favours the aggregation of the nanotubes at high loadings. In contrast the two-dimensional f-Ge structure enhanced the mechanical response when using higher loading of this filler. This explanation is confirmed by the nanocomposites crystal properties. The nanocomposites reinforced with graphene showed the highest crystallinity and lowest crystal perfection due to the nucleation provided by the better dispersion of this nanomaterial in the polymer matrix.

Acknowledgments

References

[1]   Martínez-Hernández, Velasco-Santos C and Castaño V M 2010 Carbon nanotubes composites: Processing, grafting and mechanical and thermal properties *Curr Nanosc* **6** (1) 12-39.

[2]   Velasco-Santos C, Martínez-Hernández A L, Fisher F, Ruoff R and Castaño V M 2003 Dynamical–mechanical and thermal analysis of carbon nanotube–methyl-ethyl methacrylate nanocomposites J. *Phys. D: Appl. Phys.* **36** 1423-1428.

[3]   Velasco-Santos C, Martínez-Hernández A L, Fisher F T, Ruoff R and Castaño V M 2003 Improvement of thermal and mechanical properties of carbon nanotube composites through chemical functionalization *Chem Mater* **15** (23) 4470-4475.

[4]   Shen J,. Shi M, Yan B, Ma H, Li N, Hu Y et al 2010 Covalent attaching protein to graphene oxide via diimide-activated amidation *Colloids Surf., B* **81** 434–438.

[5]   Shen J, Huanga W, Wu L, Hu Y and Ye M 2007 Study on amino-functionalized multiwalled carbon nanotubes *Mater. Sci. Eng.* **464** 151-156.

[6]   Shen J, Yan B, Shi M, Ma H, N Li, Hu Y and Ye M 2011 Synthesis of graphene oxide-based biocomposites through diimide-activated amidation *J.Colloid Interface Sci.* **356** 543–549.

[7]   Chen X, Chen X, Lin M, Zhong W, Chen X and Chen Z 2007 Functionalized multi-walled carbon nanotubes prepared by in situ polycondensation of polyurethane. *Macromol. Chem. Phys.* **208** 964–972.

[8]   Wong S C, Baji A, Leng S 2008 Effect of fiber diameter on tensile properties of electrospun poly(ε-caprolactone) *Polymer* **49** (21) 4713-4722.

[9]   Baji A, Mai Y, Wong S C, Abtahi M and Chen P 2010 Electrospinning of polymer nanofibers: effects on oriented morphology, structures and tensile properties *Compos. Sci. Technol.* **70** (5) 703-718.

[10]   Park S, An J, Piner R D, Jung I, Yang D, Velamakanni A, et al 2008 Aqueous suspension and characterization of chemically modified graphene sheets *Chem Mater* **20** (21) 6592-6594.

[11]   Shen X, Jiang L, Ji Z, Wu J, Zhou H, Zhu G 2011Stable aqueous dispersions of graphene prepared with hexamethylenetetramine as a reductant. *J. Colloid Interface Sc*i. **354** (2) 493-497.

[12]   Datsyuk V, Kalyva M, Papagelis K, Parthenios J, Tasis D, Siokou A, et al 2008 Chemical oxidation of multiwalled carbon nanotubes *Carbon*, **46** (6) 833-840.

[13]   Ferrari A C and Robertson J 2000 Interpretation of raman spectra of disordered and amorphous carbon *Phys Rev B* **61** (20) 14095-14107.

[14]   Jog J P 2006 Crystallisation in polymer nanocomposites *Mater Sci Technol* **22** (7) 797-806.

[15]   Chavarria F and Paul D R 2004 Comparison of nanocomposites based on nylon 6 and nylon 66 *Polymer* **45** (25) 8501-8515.

[16]   Lu Y, Zhang Y, Zhang G, Yang M, Yan S, Shen D 2004 Influence of thermal processing on the perfection of crystals in polyamide 66 and polyamide 66/clay nanocomposites *Polymer* **45** (26) 8999-9009.